A multilinear direction finding (DF) approach for a sensor-array with multiple scales of invariance

Sebastian Miron, Yang Song, David Brie, Kainam Thomas Wong

▶ **To cite this version:**

Sebastian Miron, Yang Song, David Brie, Kainam Thomas Wong. A multilinear direction finding (DF) approach for a sensor-array with multiple scales of invariance. 2013. hal-00992223

HAL Id: hal-00992223
https://hal.science/hal-00992223

Submitted on 16 May 2014

HAL is a multi-disciplinary open access archive for the deposit and dissemination of scientific research documents, whether they are published or not. The documents may come from teaching and research institutions in France or abroad, or from public or private research centers.

L'archive ouverte pluridisciplinaire **HAL**, est destinée au dépôt et à la diffusion de documents scientifiques de niveau recherche, publiés ou non, émanant des établissements d'enseignement et de recherche français ou étrangers, des laboratoires publics ou privés.

A multilinear direction finding (DF) approach for a sensor-array with multiple scales of invariance

Sebastian Miron, Yang Song, David Brie and Kainam Thomas Wong

Abstract

In this paper, we introduce a novel direction finding algorithm for a multi-scale sensor-array, that is, an array presenting multiple scales of invariance. We show that the collected data can be represented as a Candecomp/Parafac (CP) model, for which we analyze the identifiability properties. A two-stage algorithm for direction-of-arrival (DOA) estimation with such an array is also proposed. This approach generalizes the results given in [1] to an array that presents an arbitrary number of spatial invariances. We illustrate, on a particular array geometry, that our method outperforms the ESPRIT-based approach introduced in [2]. Moreover, we show that the single-snapshot case can be handled by our method, provided that the array includes at least three scale-levels.

Index Terms

direction finding, DOA estimation, Candecomp/Parafac decomposition, multi-scale array

I. Introduction

High-resolution techniques such as MUSIC [3], [4] or ESPRIT [5] introduced in the late '70s and the '80s, gave a new lease of life to sensor-array signal processing. An important number of eigenstucture-based direction finding (DF) algorithms have been proposed since, for various types of sensors and array configurations. In [1], Sidiropoulos *et al.* proposed for the first time a DOA estimation approach based on a CP model of the data, and highlighted the link between CP and ESPRIT. Over the next years, several other authors came up with CP-based DF algorithms for *scalar*-sensor or *vector*-sensor arrays. Liang *et al.* [6] proposed a cumulant-based algorithm for 4D near-field source localization using the CP model. DOA-estimation algorithms for vector sensor arrays were developed in [7] and[8], based on a three-way CP model, for which an identifiability analysis was provided in [9]. A similar approach,

S. Miron (sebastian.miron@univ-lorraine.fr) and D. Brie (david.brie@univ-lorraine.fr) are with Centre de Recherche en Automatique de Nancy (CRAN), UMR 7039, Université de Lorraine, Vandœuvre, F-54506, France. They are supported by the PHC PROCORE grant #26408PK.

Y. Song (yang.song@connect.polyu.hk) and K. T. Wong (ktwong@ieee.org) are with Hong Kong Polytechnic University, Hong-Kong. K. T. Wong is supported by the "France / Hong Kong Joint Research Scheme" grant #3-ZG84, and by The Hong Kong Polytechnic University grants #G-YJ50 and #G-YL81.

exploiting the quadrilinear structure of the data covariance, was proposed in [10], while Gong [11] developed a trilinear cross-covariance DF method for an array of electric tripoles. Nion and Sidiropoulos established in [12] a CP approach for source detection and localization in MIMO radar systems. In [13], a regularized CP-based approach is used to solve the DOA estimation problem with a single six-component electromagnetic antenna. Recently, Zhang *et al.* proposed in [14] an algorithm for coherent angle estimation for bistatic MIMO radar based on a CP model with linear dependences (PARALIND). Orthogonal tensor decompositions (*e.g.* HOSVD, HOEVD) have also been used in the last years to build up DF algorithms (see *e.g.* [15], [16], [17], [18] an the references therein).

The approach proposed in this paper generalizes and extends the philosophy introduced in [1] an array presenting multiple scales of invariance. The main idea is to use an array geometry for which the source steering vectors can be expressed as N-way tensor products. A somewhat similar idea, but in a different context, was used in [19]. However, the authors of [19] utilized various tensor decompositions of a 2D array grid with two levels of spatial invariance, to illustrate their effect on coherent source estimation performance. In this paper, we propose a DF algorithm for any 3D sensor array with an arbitrary number of scales of invariance and provide an efficient two-stage DOA estimation algorithm that exploits all the available information on the sources' DOAs. It is worth noting that the concept of *multi-scale array* used in this paper is totally different from that of *nested arrays* introduced in [20], where the main idea is to exploit the associated "difference co-array" to resolve more sources than physical sensors.

The remainder of this paper is organized as follows: section II presents the proposed multi-scale array configuration; the corresponding data model is derived in section III. In section IV, we analyze the identifiability of the proposed data model and a two-stage algorithm for DOA parameter estimation is introduced in section V. In section VI, the proposed method is compared in simulations to the ESPRIT-based approach in [2]; conclusions are drawn in section VII.

II. The geometric configuration of a multiple scale-invariant sensor array

We introduce in this section the configuration of the array for which the data model is to be derived in section III. Consider an subarray composed of L_1 omnidirectional identical sensors indexed by $l_1 = 1, \ldots, L_1$. Consider then, L_2 identical replicas of this subarray, spatially translated to arbitrary, possibly known locations. The L_2 different copies of the subarray, indexed by $l_2 = 1, \ldots, L_2$, can now be seen as *subarrays* of a larger (*higher-level*) array. The proposed array structure can be further developed by considering an additional level, composed of L_3 translated replicas of the previous $L_1 L_2$ sensors array, indexed by $l_3 = 1, \ldots, L_3$. Let us generalize this scheme to a total of N such hierarchical levels, the "highest" level consisting of L_N subarrays indexed by $l_N = 1, \ldots, L_N$. It is worth noting that two different subarrays at a given level n need not be disjoint, *i.e.* they may have in common subarrays/sensors of the previous level $(n-1)$. However, if all subarrays at all levels are disjoint, then the entire array contains a total number of $L = L_1 L_2 \ldots L_N$ identical sensors. Fig. 1 illustrates a three-level array with co-planar sensors.

Consider also a Cartesian coordinate system $OXYZ$ attached to the considered array. An impinging source is

characterized in this coordinate system by its direction-cosines u, v, w :

$$\begin{bmatrix} u \\ v \\ w \end{bmatrix} = \begin{bmatrix} \sin\theta\cos\phi \\ \sin\theta\sin\phi \\ \cos\theta \end{bmatrix}, \tag{1}$$

where $\theta \in [0, \pi[$ denotes the source elevation angle measured from the vertical Z-axis and $\phi \in [0, 2\pi[$ symbolizes the azimuth angle measured from the positive X-axis.

Let us consider a single level-1 subarray. In the coordinate system $OXYZ$, the position of the l_1th sensor of this subarray is given by the vector $(x_{l_1}^{(1)}, y_{l_1}^{(1)}, z_{l_1}^{(1)})$. Consider next L_1 such subarrays. The position of the l_1th sensor of the l_2th subarray is given by $(x_{l_1}^{(1)} + x_{l_2}^{(2)}, y_{l_1}^{(1)} + y_{l_2}^{(2)}, z_{l_1}^{(1)} + z_{l_2}^{(2)})$, where $(x_{l_2}^{(2)}, y_{l_2}^{(2)}, z_{l_2}^{(2)})$ indicates the spatial displacement of the l_2th subarray with respect to the first subarray. It can be easily shown by induction that, for a N-level array, the position of one sensor is given by $(x_{l_1}^{(1)} + \cdots + x_{l_N}^{(N)}, y_{l_1}^{(1)} + \cdots + y_{l_N}^{(N)}, z_{l_1}^{(1)} + \cdots + z_{l_N}^{(N)})$, where $(x_{l_N}^{(N)}, y_{l_N}^{(N)}, z_{l_N}^{(N)})$ indicates the spatial displacement of the l_Nth subarray compared to the first subarray of the level N (indexed by $l_N = 1$), *etc.*.

The presented array structure is composed by sensor/subarrays "packs" that differ from each others only by a translation in the three-dimensional Euclidian space. This provides interesting spatial invariance properties for the data acquired by this array, as shown in the next section.

III. Data Model

Consider first a narrow-band plane wave impinging on the array described in section II. Let us symbolize by $a_{l_1 l_2 \ldots l_N}$ its phase factor at sensor indexed by $l_1, l_2, \ldots, l_N$ at the N different array levels, respectively and denote $\mathbf{k} = [u\ v\ w]^T$ and $\mathbf{d}_{l_n}^{(n)} = [x_{l_n}^{(n)}\ y_{l_n}^{(n)}\ z_{l_n}^{(n)}]^T$, with $n = 1, \ldots, n$. With the notations introduced above, the phase factor is given by :

$$a_{l_1 l_2 \ldots l_N}(\mathbf{k}) = \exp\left\{ j\frac{2\pi}{\lambda} \sum_{n=1}^{N} \mathbf{k}^T \mathbf{d}_{l_n}^{(n)} \right\} = \prod_{n=1}^{N} \exp\left\{ j\frac{2\pi}{\lambda}\, \mathbf{k}^T \mathbf{d}_{l_n}^{(n)} \right\}. \tag{2}$$

Thus, the array manifold for the entire sensor array is

$$\mathbf{a}(\mathbf{k}) = \mathbf{a}_1(\mathbf{k}) \otimes \cdots \otimes \mathbf{a}_N(\mathbf{k}), \tag{3}$$

with

$$\mathbf{a}_n(\mathbf{k}) = \begin{bmatrix} e^{j(2\pi/\lambda)\mathbf{k}^T \mathbf{d}_1^{(n)}} \\ \vdots \\ e^{j(2\pi/\lambda)\mathbf{k}^T \mathbf{d}_{L_n}^{(n)}} \end{bmatrix} \tag{4}$$

an $L_n \times 1$ vector, $n = 1, \ldots, N$ and " $\otimes$ " the Kronecker product of two matrices.

Next, consider P narrow-band, plane-waves, having traveled through a nonconductive homogeneous isotropic medium, impinging upon the array from directions $\mathbf{k}_p = [u_p\ v_p\ w_p]^T$, with $p = 1, \ldots, P$. Denote by $s_p(t)$ the

time signal emitted by the pth narrow-band source[1]. Then, the output at time t of the entire sensor array can be expressed as an $L \times 1$ vector

$$\mathbf{z}(t) = \sum_{p=1}^{P} \Big(\mathbf{a}_1(\mathbf{k}_p) \otimes \cdots \otimes \mathbf{a}_N(\mathbf{k}_p) \Big) s_p(t) + \mathbf{n}(t), \tag{5}$$

where $\mathbf{n}(t)$ is a complex-valued zero-mean additive white noise.

Let us assume that we have at our disposal K snapshots at time instants $t_1, t_2, \ldots, t_K$, and define the following matrices :

$$\mathbf{A}_1 = \Big[\mathbf{a}_1(\mathbf{k}_1), \ldots, \mathbf{a}_1(\mathbf{k}_P) \Big] \ (L_1 \times P) \tag{6}$$

$$\vdots$$

$$\mathbf{A}_N = \Big[\mathbf{a}_N(\mathbf{k}_1), \ldots, \mathbf{a}_N(\mathbf{k}_P) \Big] \ (L_N \times P) \tag{7}$$

and

$$\mathbf{S} = \begin{bmatrix} s_1(t_1) & s_2(t_1) & \ldots & s_P(t_1) \\ s_1(t_2) & s_2(t_2) & \ldots & s_P(t_2) \\ \vdots & \vdots & \ddots & \vdots \\ s_1(t_K) & s_2(t_K) & \ldots & s_P(t_K) \end{bmatrix} = \Big[\mathbf{s}_1, \ \mathbf{s}_2, \ldots, \mathbf{s}_P \Big] \ (K \times P). \tag{8}$$

The collection of K snapshots of the array can then be organized into an $L \times K$ data matrix as

$$\mathbf{Z} = [\mathbf{z}(t_1), \ldots, \mathbf{z}(t_K)] = \Big(\mathbf{A}_1 \odot \cdots \odot \mathbf{A}_N \Big) \mathbf{S}^T + \mathbf{N}, \tag{9}$$

where "$\odot$" denotes the Khatri-Rao (Kronecker column-wise) product of two matrices, and $\mathbf{N}$ $(L \times K)$ is a complex-valued matrix modeling the sensor noise on the entire array for all K temporal snapshots. Equation (9) reveals a $(N+1)$-dimensional CP structure (see [21], [22]) of the collected data.

In the case where only one sample is available, *i.e.* matrix $\mathbf{S}$ is a $1 \times P$ vector, the data model given by (9) becomes

$$\mathbf{z} = \Big(\mathbf{A}_1 \odot \cdots \odot \mathbf{A}_N \Big) \mathbf{s} + \mathbf{n}, \tag{10}$$

with $\mathbf{z} = \mathbf{z}(t_1)$, $\mathbf{s} = \mathbf{s}(t_1) = \Big(\mathbf{S}(1,:) \Big)^T$ and $\mathbf{n} = \mathbf{N}(:,1)$. In the definitions above, we used the Matlab notations for columns and rows selection operators. Equation (10) is a vectorized representation of a N-dimensional CP data model (see *e.g.*[23] for details on the different CP representations). It is worth noting that if only one snapshot of the array is available, the $N+1$ CP model degenerates into a N-dimensional one.

[1]The incident signals are narrow-band in that their bandwidths are very small compared with the inverse of the wavefronts' transit time across the array.

IV. DATA MODEL IDENTIFIABILITY

Before presenting the proposed algorithm for source DOA estimation, a discussion on data model identifiability is required. In this paper, the term *identifiability* refers to the non-ambiguous estimation of the DOA parameters from the collected data. We will only focus herein on the identifiability conditions for the estimation of matrices $\mathbf{A}_1, \ldots, \mathbf{A}_N$ and $\mathbf{S}$, from the data (equation (9)). A brief discussion on the ambiguity problems when estimating the direction-cosines from $\mathbf{A}_1, \ldots, \mathbf{A}_N$ is provided in section V.

The main advantage of the CP model, compared to other source separation approaches, is its identifiability under only mild conditions. In [24], Kruskal derived a sufficient condition for the identifiability of the 3-way CP model. This condition is based on a special notion of matrix rank, called the *Kruskal-rank* or *k-rank*[2], and has been generalized later to N-way arrays by Sidiropoulos and Bro [25]. If applied to the data model given by eq. (9), this condition states that the matrices $\mathbf{A}_1, \ldots, \mathbf{A}_N$ and $\mathbf{S}$ can be uniquely estimated from $\mathbf{Z}$ if

$$\sum_{n=1}^{N} k_{\mathbf{A}_n} + k_{\mathbf{S}} \geq 2P + N, \tag{11}$$

where $k_{(.)}$ denotes the Kruskal-rank of a matrix. This estimation is unique up to two trivial indeterminacies. The first indeterminacy is an arbitrary simultaneous column permutation of all $N + 1$ matrices, and signifies that the order of the sources can not be *a priori* determined. The second one is an arbitrary column scaling/counterscaling and can be resolved by normalizing each column of matrices $\mathbf{A}_1, \ldots, \mathbf{A}_N$ by the modulus of that column's first element.

If the P sources have distinct DOAs and are not fully correlated, the identifiability condition (11) can be reformulated as

$$\sum_{n=1}^{N} \min(L_n, P) + \min(K, P) \geq 2P + N. \tag{12}$$

In general, the number of snapshots exceeds the number of sources ($K > P$), in which case (12) becomes

$$\sum_{n=1}^{N} \min(L_n, P) \geq P + N. \tag{13}$$

Furthermore, if $L_n > P$ for $n = 1, \ldots, N$, (this could be the case especially for small values of N), than the sufficient condition will always be met for model identifiability if $P, N \geq 2$. This means that, for non-collocated sources with not fully correlated temporal sequences, the CP model identifiability is easily achieved in practical applications.

Another case of interest is when the array has at least three scales of invariance. In this situation the model can be identified even under the single-snapshot assumption, and Kruskal's condition reads:

$$\sum_{n=1}^{N} \min(L_n, P) \geq 2P + N - 1. \tag{14}$$

Meanwhile, if the condition (11) does not hold, the identifiability of (9) can no longer be ensured. In this case, *partial identifiability* may apply, meaning that only a part of the parameters in (9) may be uniquely recovered.

[2]The Kruskal-rank of a matrix is the maximum number of independent columns that can selected from that matrix in an arbitrary manner.

Partial identifiability results for the 3-way CP model, similar to Kruskal's condition, have been derived in [26]. A generalization of these results to N-way arrays has been proposed in [27]. Specific identifiability conditions for the case of fully coherent sources and/or collocated sources could be derived from these results. However, this analysis is beyond the scope of this paper.

V. Parameter estimation

The parameter estimation procedure proposed in the paper can be split into two stages. The first stage consists of estimating the N steering vectors $\mathbf{a}_n(\mathbf{k}_p)$ $(n = 1, \ldots, N)$ for each of the P sources $(p = 1, \ldots, P)$, by exploiting the CP structure (9) of the collected data. For the first stage, an Alternating Least Squares (ALS) procedure can be used to fit the CP model. It consists of recursively estimating one of the $N + 1$ matrices $\mathbf{A}_1, \ldots, \mathbf{A}_N, \mathbf{S}$, by fixing the other N of them [21], [22]. ALS is simple to implement but suffers from a slow convergence rate and is sensitive to over- (and under-) factoring. Improved versions of this algorithm, using data compression and line search techniques that partly mitigate these deficiencies, have been proposed in [28], [29], [30]. Derivative-based methods or direct (non-iterative) procedures can likewise be employed to fit the CP model [31]. Such CP decomposition methods have been implemented in Matlab and are freely available online (see *e.g.* [32], [33]). This present paper's simulations will use the COMFAC approach of [29].

The second stage estimates the source direction-cosines $\mathbf{k}_p$, $p = 1, \ldots, P$ from the steering vectors obtained at the previous stage. To this end, we propose a sequential procedure that exploits all the available information from the source steering vectors of all scale levels.

Define the following cost functions:

$$\mathcal{J}_n(\mathbf{k}_p) = \|\hat{\mathbf{a}}_n^p - \mathbf{a}_n(\mathbf{k}_p)\|^2, \text{ with } n = 1, \ldots, N, \tag{15}$$

where $\hat{\mathbf{a}}_n^p$ denotes the nth level estimated steering vector for the pth source. Estimating the DOA parameters for the pth source comes down to minimizing the following criterion:

$$\mathcal{I}_N(\mathbf{k}_p) = \sum_{n=1}^{N} \mathcal{J}_n(\mathbf{k}_p). \tag{16}$$

This function is non-convex and highly non-linear with respect to the direction-cosines; hence a direct local optimization procedure would fail in most cases. We propose a sequential strategy to minimize $\mathcal{I}_N(\mathbf{k}_p)$, using an iterative refinement of the direction-cosine estimates. The method is based on the fact that, when noise-free, the N cost-functions in (15) have the same global minimum.

Assume that the level-1 subarrays' inter-sensor separations would not exceed half a wavelength. This assumption is essential to obtaining a set of high-variance but unambiguous direction-cosine estimates. On the contrary, the spatial displacement between any two subarrays of the highest level is supposed to exceed $\lambda/2$, where λ is the wavelength. This will produce lower variance but cyclically ambiguous estimates for the same set of direction-cosines. Under the first assumption, the $\mathcal{J}_1(\mathbf{k}_p)$ function is unimodal inside the support region of the DOA parameters. Therefore, any local optimization procedure should converge towards the global minimum for the criterion. Thus, we obtain a

set of high-variance, but unambiguous, estimates of the DOA parameters, to be denoted by $\mathbf{k}_{p,1}^*$ with $p = 1, \ldots, P$. These values will subsequently be used, in a second step, as the initial point for the minimization of

$$\mathcal{I}_2(\mathbf{k}_p) = \mathcal{J}_1(\mathbf{k}_p) + \mathcal{J}_2(\mathbf{k}_p). \tag{17}$$

As no assumption is made on the distances between the level-2 subarrays, $\mathcal{I}_2(\mathbf{k}_p)$ may present more than one local minimum. Hence, a good initial point is crucial for the optimization procedure. The estimates obtained by the minimization of $\mathcal{I}_2(\mathbf{k}_p)$, denoted by $\mathbf{k}_{p,2}^*$, are then used for the minimization of $\mathcal{I}_3(\mathbf{k}_p) = \sum_{n=1}^{3} \mathcal{J}_n(\mathbf{k}_p)$, and so on, until the final estimates are obtained by the minimization of $\mathcal{I}_N(\mathbf{k}_p)$. We emphasize the necessity of sequential iteration for good results, going from level n to level $n+1$. A direct "jump" from a low hierarchical level (*e.g.* level 1) to a high hierarchical level (*e.g.* level N) may result in erroneous results, especially for low signal-to-noise ratios (SNR). The reason is that the number of local minima for $\mathcal{J}_n(\mathbf{k})$ and $\mathcal{I}_n(\mathbf{k})$ increases with n and that the low-level estimates have a high variance. Thus, the direct initialization of a high-level parameter estimation step with a low-level estimate may result in convergence towards a local minimum instead of the global one.

This sequential minimization can be regarded as a Graduated Non-Convexity (GNC) optimization approach [34], in which the multi-scale array geometry determines the parameter controlling the transformation of the initial convex problem into a non-convex problem. A sufficient condition ensuring the global minimization of the non-convex problem is that:

- the global minimum of the initial convex problem can be reached;
- the global minimum of each intermediate sub-problem belongs to the locally convex region around the global minimum of the subsequent optimization problem.

The first requirement is met because the inter-element spacing of the level-1 subarray is $\leq \lambda/2$, resulting in a uni-modal criterion $\mathcal{J}_1(\mathbf{k})$. Regarding the second requirement, it is difficult to determine whether it is met, because the shape of the criterion $\mathcal{J}_N(\mathbf{k})$ depends on the array geometry. However, as the number of local minima increases with the inter-sensor spacing, the algorithm would likely reach the global minimum of the criterion $\mathcal{J}_N(\mathbf{k})$ provided that the inter-sensor spacing of the successive scales of the array do not change excessively from one level to another level.

The proposed algorithm can be summarized as follows:

THE TWO-STAGE ESTIMATION ALGORITHM

First Stage: Estimate $\mathbf{A}_1, \ldots, \mathbf{A}_N$ by CP decomposition of the data $\mathbf{Z}$ or $\mathbf{z}$ (see eq. (9) or (10)).

Second Stage:

- For $p = 1, \ldots, P$ and

for $n = 1, \ldots, N$ compute

$$\mathbf{k}^*_{p,n} = \underset{\mathbf{k}_p}{\operatorname{argmin}}\, \mathcal{I}_n(\mathbf{k}_p) = \underset{\mathbf{k}_p}{\operatorname{argmin}} \sum_{i=1}^{n} \mathcal{J}_i(\mathbf{k}_p). \tag{18}$$

- *Output:* The estimated parameters for the P sources: $\hat{\mathbf{k}}_p = (\hat{u}_p, \hat{v}_p, \hat{w}_p) = \mathbf{k}^*_{p,N}$ with $p = 1, \ldots, P$.

In this paper, the first stage is performed using the COMFAC CP-fitting algorithms implemented in the Matlab toolbox [32]. For the second stage, the minimization of $\mathcal{I}_n$ in (18) is done by the Nelder-Mead simplex algorithm, initialized by the estimates of the previous step $\mathbf{k}^*_{p,n-1}$. Random values, within the parameters definition domain, are used to initialize the minimization of $\mathcal{I}_1 = \mathcal{J}_1$.

The next section will illustrate the performance of the proposed algorithm in numerical simulations.

VI. Simulation results and discussion

In this section, we compare our approach with the one developed by Wong and Zoltowski in [2], using an array configuration proposed by those same authors. The Cramér-Rao Bound (CRB) for the considered model, derived in the appendix, is used as a benchmark. The sensor array consists of a 2×2 square grid at an extended spacing of $10\ \lambda$ and a 5-element half-wavelength spaced cross-shaped subarray at each grid point, as illustrated by Fig. 2. This array can be seen as having two hierarchical levels with $L_1 = 5$ sensors and $L_2 = 4$ subarrays, or as a three-level array with $L_1 = 5, L_2 = 2$ and $L_3 = 2$. In [2], the source' DOAs are estimated using an ESPRIT-based technique. Two types of estimates (coarse but unambiguous, versus fine but cyclically ambiguous) are computed separately for each of the x and y axes of the considered spatial grid, using four matrix pencils altogether. The coarse but unambiguous estimates are then used to disambiguate the fine but cyclically ambiguous DOA estimates. This procedure is followed by a pairing step of the x-axis and y-axis direction-cosines of the sources.

The considered signal scenario involves two equal-power narrowband source signals impinging respectively from $(u_1 = 0.83, v_1 = 0.17)$, and $(u_2 = 0.13, v_2 = 0.79)$. There are $I = 500$ independent Monte-Carlo runs for each data point plot on the figures. The additive white noise is complex-value Gaussian distributed. All figures plot the "composite root-mean-square-error" (CRMSE) of the sources' Cartesian direction-cosine estimates, versus SNR. This CRMSE is defined as

$$\frac{1}{I} \sum_{i=1}^{I} \sqrt{\frac{\delta^2_{u,p,i} + \delta^2_{v,p,i}}{2}}, \tag{19}$$

where $\delta_{u,p,i} (\delta_{v,p,i})$ symbolizes the error in estimating the pth source's x-axis (y-axis) direction-cosine during the ith run.

The pth source signal model used for the simulations represented on Fig.3-6 is:

$$s_p(t) \quad = \quad a_p(t)\ e^{j\left(2\pi \frac{f_p}{3} t + \varphi_p\right)}, \tag{20}$$

where $a_p(t)$ is a zero-mean unit-variance complex-value random time series Gaussian distributed and temporally white, φ_p is a random variable uniformly distributed between $[0, 2\pi]$ and $f_1 = f_2 = 1$. In Figures 3-5 the two

complex signals ($a_1(t)$ and $a_2(t)$) are not correlated. All random entities are otherwise statistically independent from each other.

A first experiment evaluates the performance of the two algorithms for different SNR's in the case of uncorrelated sources. Figures 3(a) and 3(b) plot the CRMSE for $K = 5$ and $K = 20$ snapshots, respectively. For high SNR, the two approaches yield similar results, very close to the CRB, while at low SNR, the proposed algorithm outperforms ESPRIT. This phenomenon is more obvious for small values of K and can be explained by the fact that our method also estimates the time sequences for the impinging waves. This is not the case for the method in [2], that averages over the time dimension to estimate the data covariance matrix. Thus, the total number of parameters estimated by CP equals $(L_1 + L_2 + K)P$ while the number of parameters for ESPRIT is L_1L_2P. Roughly speaking, one of the situations where our algorithm provides better results is when the number of parameters to estimate is smaller compared to other method, *i.e.* for small values of K. Figure 4 illustrates this statement using different numbers of snapshots $K = \{2, 3, \ldots, 19, 20, 30, 40, \ldots, 90, 100\}$ for an SNR of 15 dB. It can be observed that the multi-scale CP approach produces more accurate results for a number of snapshots smaller that about $K = 11$, which agrees with the simplified analysis above.

The second experiment illustrates the fact that the proposed algorithm can be applied even if only a single snapshot is available. However, in this case, the $(N + 1)$-way CP model degenerates into an N-dimensional one, as shown by equation (10). Therefore, the array depicted on Fig.2 is now seen as a 3-level array, where the first level is the 5-element cross-shaped subarray ($L_1 = 5$), the second level is composed of two of such configurations, aligned along the x-axis ($L_2 = 2$) and the third level is the couple of two level-2 subarrays ($L_3 = 2$). Figure 5 plots the results for the two methods under the single-snapshot scenario. It can be seen that the proposed method still yields fair results, while ESPRIT is unusable here.

In a third experiment, we study the behavior of the two approaches in the presence of correlated sources. For that, we simulated two sources with a correlation coefficient of 0.83 between $a_1(t)$ and $a_2(t)$. The numerical simulation results are plotted on Figure. 6. Once more, the proposed algorithm outperforms the ESPRIT method. This is because, in this case, the source covariance matrix is no longer diagonal, which violates a restriction in the model used in [2] while entirely allowed by our CP approach. However, a strong correlation between sources may yield convergence problems for our algorithm, especially for a low SNR and a small number of snapshots, as one can see on Fig. 6(a).

We show in this section that, for the given array configuration, the proposed approach provides more accurate results than the method in [2], in diverse scenarios. However, this comes at the expense of a smaller number of sources that can be, in general, estimated by our method. For a $Q_1 \times Q_2$ grid of 5-element half-wavelength spaced

cross-shaped subarrays, the approach in [2] can handle only up to

$$P \leq \min\{5(Q_1-1)Q_2-1, 5Q_1(Q_2-1)-1, 2Q_1Q_2-1\} \tag{21}$$

uncorrelated sources, while the number of sources P that can be handled by our approach is given by

$$\min(5,P)+\min(Q_1Q_2,P)+\min(K,P) \geq 2P+2. \tag{22}$$

For the array configuration used in this section, both approaches can handle up to 7 sources, but if the size of the grid increases, the number of sources that can be estimated by ESPRIT increases.

Another drawback of the proposed method is the computational burden which is, in general, bigger than for ESPRIT. However, powerful CP fitting algorithms [29], [31] have been developed in the last years and they significantly improve the convergence speed. Moreover, closed-form solutions exist for CP decompositions [35] that are particularly efficient for Vandermonde structured data [36], [37] (which frequently appears in array processing), and present a computational complexity equivalent to ESPRIT's. Nevertheless, for the approach in [2], two pairing procedures (that may fail for difficult scenarios), are necessary for the identification of the source parameters. This pairing is no longer needed with our method, as it is intrinsic to the CP decomposition.

VII. Conclusions

This paper introduces a new sensor-array configuration for DOA estimation based on a scale invariance principle; and we proved that the data acquired by this array follows a multidimensional CP structure. Our analysis proves that this model is identifiable, under only mild conditions that are readily met in practical applications. A two-stage algorithm for the estimation of the source DOAs with such an array was proposed and compared with an ESPRIT-based approach developed in [2]. Our Monte Carlo simulations verify that our proposed method outperforms in terms of root mean-square error an earlier ESPRIT-based approach [2], especially for a small number of snapshots or for time correlated sources. Moreover, unlike the ESPRIT-based approach, this proposed algorithm can also be applied in the single-snapshot scenario and is not limited to rectangular array configurations.

Appendix
Derivation of Cramér-Rao Bound for the Data Model in Section VI

The K snapshots, collected by the L-element array using a sampling period T_s, can be written as

$$\mathbf{z} = \left[\mathbf{z}(T_s)^T, \cdots, \mathbf{z}(KT_s)^T\right]^T = \sum_{p=1}^{P} \mathbf{s}_p \otimes \mathbf{a}(\mathbf{k}_p) + \underbrace{\left[\mathbf{n}(T_s)^T, \cdots, \mathbf{n}(KT)_s)^T\right]^T}_{\stackrel{\text{def}}{=}\mathbf{n}}, \tag{23}$$

where $\mathbf{s}_p = [s_p(T_s), \cdots, \mathbf{s}_p(KT_s)]^T$, $\otimes$ symbolizes the Kronecker product and $\mathbf{n}$ represents a $LK \times 1$ noise vector. All deterministic unknown entities are collected into a $2P \times 1$ vector $\boldsymbol{\psi} = [u_1, \ldots, u_P, v_1, \ldots, v_P]$.

The resulting Fisher Information Matrix $\mathbf{J}$ has its (i,j)th entry equal to (equation (8.34) in [38]) :

$$[\mathbf{J}(\boldsymbol{\psi})]_{i,j} \quad = \quad K \ \mathrm{Tr}\left[\mathbf{R}_{zz}^{-1}\frac{\partial \mathbf{R}_{zz}}{\partial [\boldsymbol{\psi}]_i}\mathbf{R}_{zz}^{-1}\frac{\partial \mathbf{R}_{zz}}{\partial [\boldsymbol{\psi}]_j}\right], \tag{24}$$

where $\mathbf{R}_{zz}$ represents the data spatial covariance matrix and $\mathrm{Tr}[.]$ symbolizes the matrix trace operator.

The received data's spatial covariance matrix at a given time instant kT_s is given by

$$\mathbf{R}_{zz} \stackrel{\text{def}}{=} E\{\mathbf{z}(kT_s)\mathbf{z}(kT_s)^H\} = \mathbf{\Gamma}_{ss} + \mathbf{\Gamma}_{nn}, \tag{25}$$

where

$$\mathbf{\Gamma}_{ss} \stackrel{\text{def}}{=} E\left\{\left(\sum_{p=1}^{P} s_p(kT_s) \otimes \mathbf{a}_p(\mathbf{k}_p)\right)\left(\sum_{p=1}^{P} s_p(kT_s) \otimes \mathbf{a}_p(\mathbf{k}_p)\right)^H\right\}, \tag{26}$$

$$\mathbf{\Gamma}_{nn} \stackrel{\text{def}}{=} E\left\{\mathbf{n}(kT_s)\mathbf{n}(kT_s)^H\right\} = \sigma_n^2\mathbf{I}_L, \tag{27}$$

respectively denote the sources' and noise's spatial covariance matrices, with noise's variance as σ_n^2, and $\mathbf{I}_L$ symbolizes an $L \times L$ identity matrix.

1) For two *un*correlated zero-mean unit-variance complex Gaussian signals (Fig. 3 - 5),

$$\mathbf{\Gamma}_{ss} = \sum_{p=1}^{2} \sigma_p^2 \mathbf{a}_p \mathbf{a}_p^H, \tag{28}$$

with the pth source's variance as σ_p^2.

2) For two *cross*-correlated zero-mean unit-variance complex Gaussian signals with a correlation coefficient ρ (Fig. 6),

$$\mathbf{\Gamma}_{ss} = \rho\sigma_1\sigma_2\left(\mathbf{a}_1\mathbf{a}_2^H + \mathbf{a}_2\mathbf{a}_1^H\right) + \sum_{p=1}^{2} \sigma_p^2 \mathbf{a}_p \mathbf{a}_p^H.$$

REFERENCES

[1] N. D. Sidiropoulos, R. Bro, and G. B. Giannakis, "Parallel factor analysis in sensor array processing," *IEEE Trans. Signal Process.*, vol. 48, no. 8, pp. 2377–2388, Aug. 2000.

[2] K. T. Wong and M. D. Zoltowski, "Direction-finding with sparse rectangular dual-size spatial invariance arrays," *IEEE Trans. Aerosp. Electron. Syst.*, vol. 34, no. 4, pp. 1320–1336, Oct. 1998.

[3] G. Bienvenu and L. Kopp, "Principe de la goniométrie passive adaptative," in *Proc. 7° Colloque sur le traitement du signal et des images, GRETSI*, Nice, France, 1979.

[4] R. O. Schmidt, "A signal subspace approach to multiple emitter location and spectral estimation," Ph.D. dissertation, Stanford Univ., Stanford, CA, 1981.

[5] R. Roy and T. Kailath, "Esprit-estimation of signal parameters via rotational invariance techniques," *IEEE Trans. Acoust., Speech, Signal Process.*, vol. 37, no. 7, pp. 984 – 995, Jul. 1989.

[6] J. Liang, S. Yang, J. Zhang, L. Gao, and F. Zhao, "4D near-field source localization using cumulant," *EURASIP J. Appl. Signal Process.*, vol. 2007, no. 1, Jan. 2007.

[7] X. Guo, S. Miron, and D. Brie, "Three-way array analysis on polarized signals for direction-finding and blind source separation," in *Proc. IAR 2007*, Grenoble, France, Nov. 2007.

[8] X. Zhang and D. Xu, "Deterministic blind beamforming for electromagnetic vector sensor array," *Progress In Electromagnetics Research*, vol. 84, pp. 363–377, 2008.

[9] X. Guo, S. Miron, D. Brie, S. Zhu, and X. Liao, "A CANDECOMP/PARAFAC perspective on uniqueness of DOA estimation using a vector sensor array," *IEEE Trans. Signal Process.*, vol. 59, no. 7, pp. 3475–3481, Jul. 2011.

[10] S. Miron, X. Guo, and D. Brie, "DOA estimation for polarized sources on a vector-sensor array by PARAFAC decomposition of the fourth-order covariance tensor," in *Proc. EUSIPCO*, Lausanne, Switzerland, Aug. 2008.

[11] X. Gong, "Source localization via trilinear decomposition of cross covariance tensor with vector-sensor arrays," in *Proc. 2010 Seventh International Conference on Fuzzy Systems and Knowledge Discovery (FSKD 2010)*, Yantai, Shandong, China, Aug. 2010.

[12] D. Nion and N. Sidiropoulos, "A PARAFAC-based technique for detection and localization of multiple targets in a MIMO radar system," in *Proc. of IEEE International Conference on Acoustics, Speech and Signal Processing 2009*, Taipei, Apr. 2009, pp. 2077–2080.

[13] X.-F. Gong, Z.-W. Liu, and Y.-G. Xu, "Regularised parallel factor analysis for the estimation of direction-of-arrival and polarisation with a single electromagnetic vector-sensor," *IET Signal Process.*, vol. 5, no. 4, pp. 390–396, Jul. 2011.

[14] X. Zhang, D. Ben, and C. Chen, "Coherent angle estimation in bistatic multi-input multi-output radar using parallel profile with linear dependencies decomposition," *IET Radar Sonar Nav.*, vol. 7, no. 8, pp. 867–874, Oct. 2013.

[15] S. Miron, N. Le Bihan, and J. I. Mars, "Vector sensor MUSIC for polarized seismic sources localization," *EURASIP J. Appl. Signal Process.*, vol. 2005, no. 1, pp. 74–84, Jan. 2005.

[16] M. Haardt, F. Roemer, and G. Del Galdo, "Higher-order SVD-based subspace estimation to improve the parameter estimation accuracy in multidimensional harmonic retrieval problems," *IEEE Trans. Signal Process.*, vol. 56, no. 7, pp. 3198–3213, Jul. 2008.

[17] X. Gong, Z. Liu, Y. Xu, and M. I. Ahmad, "Direction-of-arrival estimation via twofold mode-projection," *Signal Process.*, vol. 89, no. 5, pp. 831–842, May 2009.

[18] M. Boizard, G. Ginolhac, F. Pascal, S. Miron, and P. Forster, "Numerical performance of a tensor music algorithm based on HOSVD for a mixture of polarized sources," in *Proc. 21st European Signal Processing Conference (EUSIPCO 2013)*, Marrakech, Maroc, Sep. 2013.

[19] L.-H. Lim and P. Comon, "Blind multilinear identification," *http://arxiv.org/pdf/1212.6663v2*, 2013.

[20] P. Pal and P. P. Vaidyanathan, "Nested arrays: A novel approach to array processing with enhanced degrees of freedom," *IEEE Trans. Signal Process.*, vol. 58, no. 8, pp. 4167–4181, Aug. 2010.

[21] R. A. Harshman, "Foundations of the PARAFAC procedure: Models and conditions for an 'explanatory' multimodal factor analysis," *UCLA Working Papers in Phonetics*, vol. 16, pp. 1–84, Dec. 1970.

[22] J. D. Carroll and J.-J. Chang, "Analysis of individual differences in multidimensional scaling via an N-way generalization of "Eckart-Young" decomposition," *Psychometrika*, vol. 35, no. 3, pp. 283–319, Sep. 1970.

[23] T. G. Kolda and B. W. Bader, "Tensor decompositions and applications," *SIAM Rev.*, vol. 51, no. 3, pp. 455–500, Sep. 2009.

[24] J. B. Kruskal, "Three-way arrays: Rank and uniqueness of trilinear decompositions, with application to arithmetic complexity and statistics," *Linear Algebra Applicat.*, vol. 18, no. 2, pp. 95–138, 1977.

[25] N. D. Sidiropoulos and R. Bro, "On the uniqueness of multilinear decomposition of N-way arrays," *J. Chemometr.*, vol. 14, no. 3, pp. 229–239, 2000.

[26] X. Guo, S. Miron, D. Brie, and A. Stegeman, "Uni-mode and partial uniqueness conditions for CANDECOMP/PARAFAC of three-way arrays with linearly dependent loadings," *SIAM J. Matrix Anal. Appl.*, vol. 33, no. 1, pp. 111–129, 2012.

[27] L. Zhang, T.-Z. Huang, Q.-F. Zhu, and L. Feng, "Uni-mode uniqueness conditions for CANDECOMP/PARAFAC decomposition of n-way arrays with linearly dependent loadings," *Linear Algebra Applicat.*, vol. 439, no. 7, pp. 1918–1928, Oct. 2013.

[28] R. Bro and C. A. Andersson, "Improving the speed of multiway algorithms," *Chemometr. Intell. Lab.*, vol. 42, no. 1-2, pp. 105–113, Aug. 1998.

[29] R. Bro, N. D. Sidiropoulos, and G. B. Giannakis, "A fast least squares algorithm for separating trilinear mixtures," in *Proc. Int. Workshop Independent Component Analysis and Blind Signal Separation (ICA'99)*, Aussois, France, Jan. 1999.

[30] M. Rajih, P. Comon, and R. A. Harshman, "Enhanced line search: A novel method to accelerate PARAFAC," *SIAM J. Matrix Anal. Appl.*, vol. 30, no. 3, pp. 1128–1147, Jan. 2008.

[31] G. Tomasi and R. Bro, "A comparison of algorithms for fitting the PARAFAC model," *Computational Statistics & Data Analysis*, vol. 50, pp. 1700–1734, 2006.

[32] C. A. Andersson and R. Bro, "The N-way toolbox for MATLAB," *Chemometrics and Intelligent Laboratory Systems*, vol. 52, pp. 1–4, 2000.

[33] L. Sorber, M. Van Barel, and L. De Lathauwer, *Tensorlab v1.0*. URL: http://esat.kuleuven.be/sista/tensorlab/, Feb. 2013.

[34] A. Blake and A. Zisserman, *Visual Reconstruction*, ser. Artificial Intelligence Series. MIT Press, 1987.

[35] F. Roemer and M. Haardt, "A closed-form solution for parallel factor (PARAFAC) analysis," in *Proc. ICASSP*, Las Vegas, NV, Mar. 2008, pp. 2365–2368.

[36] M. Sorensen and L. De Lathauwer, "Tensor decompositions with Vandermonde factor and applications in signal processing," in *Proc. of the Asilomar Conference on Signals, Systems and Computers*, California, USA, Nov. 2012.

[37] ——, "Blind signal separation via tensor decomposition with Vandermonde factor: Canonical polyadic decomposition," *IEEE Trans. Signal Process.*, vol. 61, no. 22, pp. 5507–5519, Nov. 2013.

[38] H. L. Van Trees, *Detection, Estimation,and Modulation Theory, Part IV: Optimum Array Processing*. New York, U.S.A.: John Wiley & Sons, Inc., 2002.

PLACE PHOTO HERE

Sebastian MIRON graduated from "Gh. Asachi" Technical University of Iasi (Romania), in 2001 and received the M.Sc. and Ph.D. degree in signal, image, and speech processing from the Institut National Polytechnique of Grenoble (France), in 2002 and 2005, respectively. He is currently a Maître de Conférence (Associate Professor) at Université de Lorraine (France), and he is conducting research at the Centre de Recherche en Automatique de Nancy (CRAN), Nancy.

S. Miron was conferred the *Best Ph.D. Award* by the Institut National Polytechnique of Grenoble in 2005. He is on the editorial board of *Physical Communication* journal since 2012.

His current research interests include vector-sensor array processing, spectroscopy and microscopy data processing, positive source separation, multidimensional signal processing and multilinear algebra.

PLACE PHOTO HERE

Yang SONG obtained his B.Eng. in communication engineering in 2007 from Zhejiang University City College (Hangzhou, Zhejiang, China), and an M.Eng. and a Ph.D. in Electronic & Information Engineering, respectively in 2008 and 2013, from the Hong Kong Polytechnic University, where he is currently a Research Associate.

His research interest lies in space-time signal processing.

PLACE PHOTO HERE

David BRIE received the Ph.D. degree in 1992 and the *Habilitation à Diriger des Recherches* degree in 2000, both from the Henri Poincaré University, Nancy (France). He is currently Full Professor at the telecommunication and network department of the Institut Universitaire de Technologie, Université de Lorraine.

He is Editor-in-chief of the *Traitement du Signal* journal since 2013.

Since 1990, he has been with the Centre de Recherche en Automatique de Nancy (France).

His research interests mainly concern inverse problems and multidimensional signal processing.

PLACE
PHOTO
HERE

Kainam Thomas WONG (SM'01), ktwong@ieee.org, earned the B.S.E. (chemical engineering) from the University of California (Los Angeles, California, U.S.A.) in 1985, the B.S.E.E. from the University of Colorado (Boulder, Colorado, U.S.A.) in 1987, the M.S.E.E. from the Michigan State University (East Lansing, Michigan, U.S.A.) in 1990, and the Ph.D. in electrical & computer engineering from Purdue University (West Lafayette, Indiana, U.S.A.) in 1996.

K. T. Wong was a Manufacturing Engineer at the General Motors Technical Center (Warren, Michigan, U.S.A.) from 1990 to 1991, and a Senior Professional Staff member at the Johns Hopkins University Applied Physics Laboratory (Laurel, Maryland, U.S.A.) from 1996 to 1998. He was a regular member of the faculty at Nanyang Technological University (Singapore) in 1998, an Assistant Professor at the Chinese University of Hong Kong in 1998-2001 and at the University of Waterloo (Canada) in 2001-2006. Since 2006, he has been with the Hong Kong Polytechnic University as an Associate Professor.

K. T. Wong was/is on the editorial boards of these journals: *Circuits, Systems, and Signal Processing* in 2007-2009, the *IEEE Signal Processing Letters* in 2006-2010, the *IEEE Transactions on Aerospace and Electronic Systems* since 2012, the *IEEE Transactions on Signal Processing* in 2008-2012, the *IEEE Transactions on Vehicular Technology* in 2007-2013, the *IET Communications* since 2013, and *Physical Communication* since 2012.

He is an elected member of the IEEE Signal Processing Society's technical committee on "sensor and multichannel processing" (SAM), for 2013-2015.

K. T. Wong's research interest includes sensor-array signal processing and signal processing for communications. He was conferred the *Premier's Research Excellence Award* by the Canadian province of Ontario in 2003.

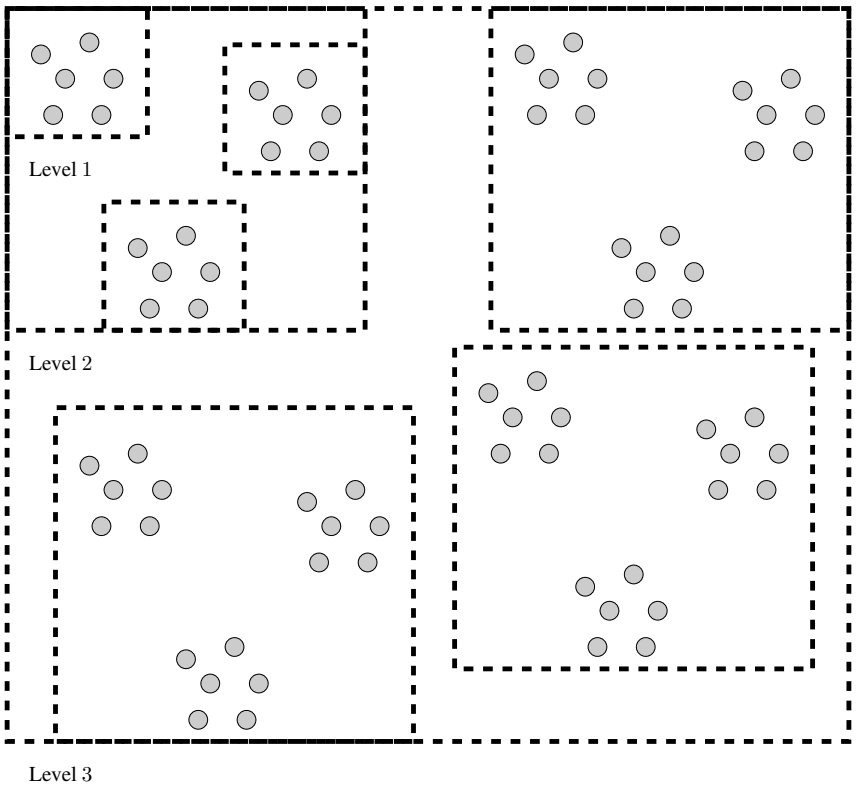

Fig. 1. A multi-scale planar array with three hierarchical levels

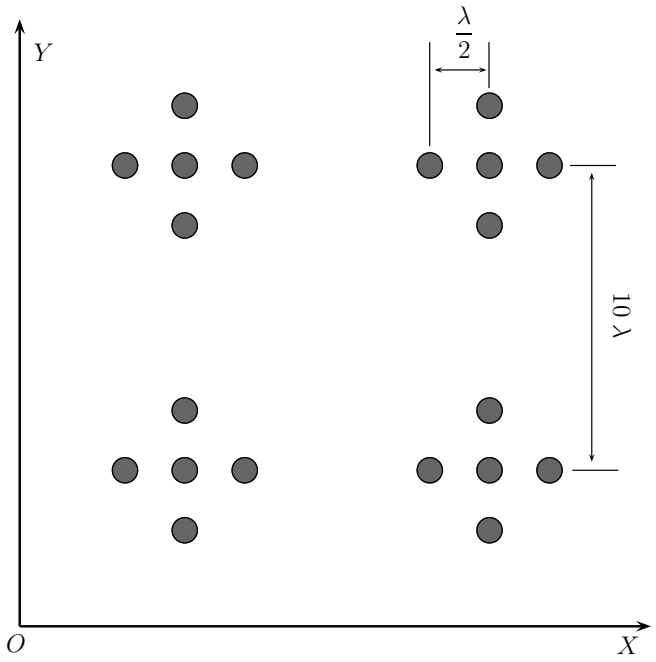

Fig. 2. The configuration of the sensor array used in the simulations

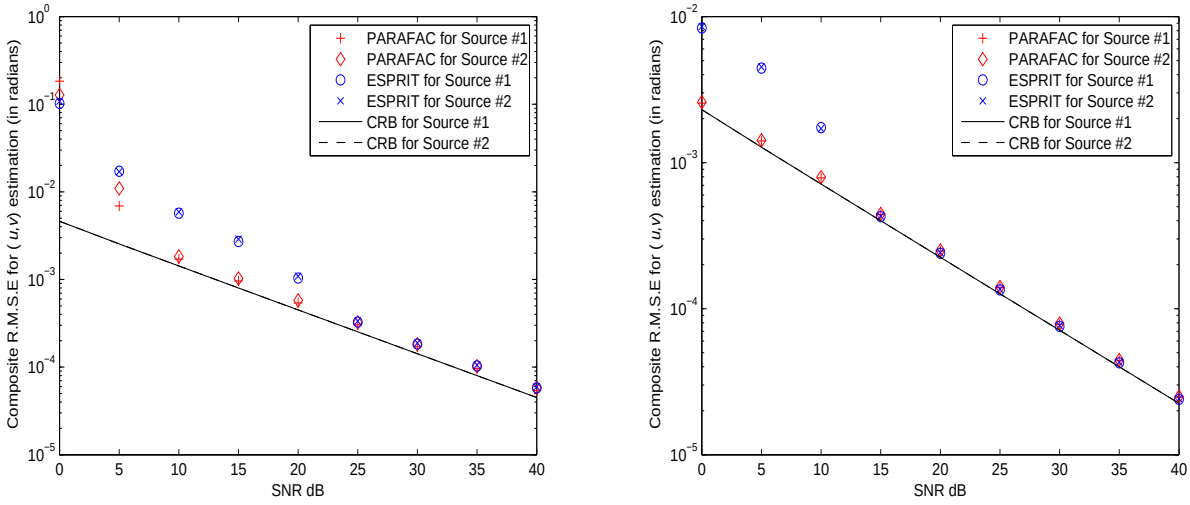

(a) $K = 5$ (b) $K = 20$

Fig. 3. Uncorrelated sources: CRMSE versus signal-to-noise power ratio (SNR).

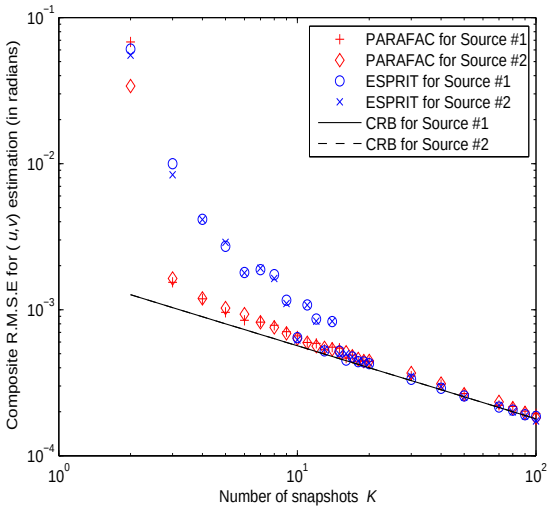

Fig. 4. Uncorrelated sources: CRMSE versus number of snapshots when SNR=15dB.

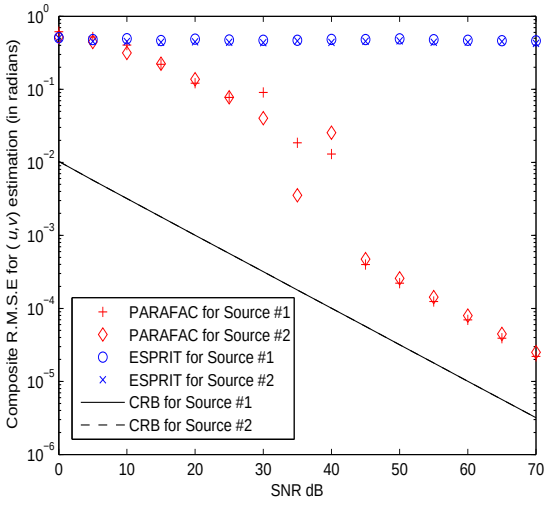

Fig. 5. Uncorrelated sources: CRMSE versus signal-to-noise power ratio (SNR) under one temporal snapshot.

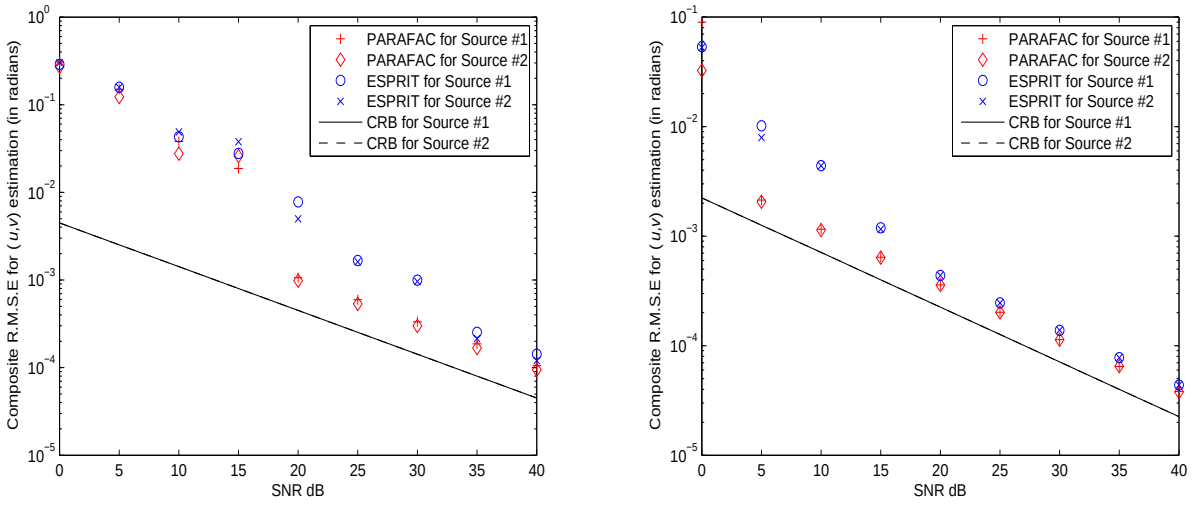

(a) $K = 5$ (b) $K = 20$

Fig. 6. Cross-correlated sources: CRMSE versus signal-to-noise power ratio (SNR).